Impact on low fibre-volume, glass/polyester rectangular plates

L. S. Sutherland and C. Guedes Soares

Abstract

Impact tests on composite plates were performed using an instrumented drop-weight machine. Orthophthalic and isophthalic resin, and different woven-roving reinforcements were considered. Degree of fibre-crimp was more influential than the type of polyester resin. Multiple, complex and interacting damage mechanisms occurred even at very low incident energies. Three main stages of damage were seen, `undelaminated', `delaminated' and `fibre damage'. Delamination gave a bi-linear force–deflection response for thicker laminates. Low fibre-crimp thinner laminates exhibited membrane stiffening, but for other thin laminates this was preceded by fibre damage. A bending and shear deflection dominated model facilitated identification and interpretation of the complex impact behaviour. For thin and undelaminated thicker laminates bending was significant. For thicker delaminated specimens shear deflection dominated. An energy balance approach successfully related impact response to impact severity. Delamination controlled almost all of the impact response of thicker laminates until fibre damage occurred.

Keywords

Low velocity impact, Impact damage, Delamination, E-glass/polyester laminates

1. Introduction

The use of reinforced plastic composite materials for marine applications promises many advantages over the use of more `conventional' materials (e.g. steel, wood, aluminium) such as ease of forming complex shapes, good environmental resistance, and high specific material properties. However, composites are known to be susceptible to impact damage, threatening to restrict the exploitation of such incentives. This impact behaviour is not well understood leading to increased safety factors and loss of potential weight savings [1]. There are two main reasons for this last point:

Firstly, the response of a composite material to impact is a highly complex dynamic event involving many interacting damage modes (e.g. internal delamination, surface micro-buckling, fibre fracture and matrix degradation [2,3]). These damage modes and paths are dependant in a complex manner on the huge number of material permutations available (e.g. fibre and resin types, quantities, architectures, and interfaces, production method [4–6]). The impact event itself is also defined by many variables such as impactor and target geometries, impact speed and energy [7,8].

Secondly, despite the large amount of work in the area the great majority of these studies concern the high-cost, high fibre-fraction, pre-impregnated carbon–fibre epoxy based, autoclave or vacuum-bag produced composites associated with the aerospace industry. The normal production method in the marine industry is the hand lay-up of E-glass reinforcement with polyester resin. This gives low fibre-fraction, variable quality `marine composites', and very little attention has been paid to the impact of these lower cost materials.

The analysis of the behaviour of an impacted laminate is usually split into two parts; the localised contact problem and the overall target deflection. Abrate [9] provides both a comprehensive review and a classification of the different areas of the problem. Hertzian contact law is usually used to model indentation at the surface [10,11]. Complete models may be used to exactly describe the deformation of the target using beam or plate theories [12,13] for simple cases for small deflections. However, these models rapidly become too computationally expensive when considering more complex architectures, large deflections or cases with significant shear deformations. They are also not effective for the consideration of damage. A more realistic approach in these latter cases is to use theories to describe the overall response of the composite such as the energy balance and spring-mass methods as described in Abrate [14], where a comprehensive overview of all of the main modelling techniques used may also be found. Recent work has attempted to further accommodate the complex damage mechanisms in terms of characterisation of the impact response and damage [3,15] and through the use of combined theoretical–empirical models [16–19].

In a marine environment, common impact events range from everyday contact with docks to collisions with floating debris and other craft, and grounding, all of which are low-velocity impacts. Recognising the impracticality of reproducing all possible scenarios, the transverse central impact of a clamped plate with a small, steel hemispherical impacter is considered here as a relatively severe case. Previous work [15,20] gave an initial insight into the impact behaviour of rectangular marine composite plates. Subsequent work [21] further characterised the impact behaviour and damage mechanisms and developed the analysis by considering the simpler case of a circular plate. However, circular panels are not common in practice and hence in the current work these characterization and analytical techniques are used to investigate the impact response of rectangular plates.

2. Experimental details

Two types of polyester resin most commonly used in the marine industry were used; the orthophthalic form, and the isophthalic form. The latter has a lower permeability to water but is also more expensive. Two weights of E-Glass woven roving (WR) reinforcement, 500 and 800 g m^{-2}, were used. The 500 g m^{-2} WR was initially supplied in a fairly coarse weave form with approximately 2.27 ends per cm, and fairly flat, wide rovings giving a low degree of crimp. However this form became unavailable and for the majority of the panels a nominally equivalent but finer weave version was used with approximately 2.85 ends per cm and narrower, more cylindrical rovings giving a higher degree of crimp. The 800 g m^{-2} WR had a similar lower degree of crimp to the coarse weave 500 g m^{-2} WR.

The same production method was used throughout the work. Cure was achieved using 1% and 2% by mass of accelerator and catalyst respectively. 3% by mass of paraffin was also added to ensure full cure of the exposed panel surface. One meter square flat panels were laid up by hand to achieve a fibre mass-fraction of 0.5 (equivalent to a fibre volume-fraction of approximately 0.35). Table 1 gives the panels laminated, with (as far as possible) equivalence of glass weight per meter squared between 500 and 800 g m^{-2} laminates. 100 mm × 150 mm rectangular specimens, with the warp aligned with the longer dimension, were then cut from the laminated panels using a diamond-surrounded circular saw. Four thickness measurements were taken, average values and coefficients of variation are given in Table 1.

Laminate	Resin	Woven Roving (gm^{-2})	Glass Weight (gm^{-2})	Average Thickness (mm)	Thickness C.O.V.
'Thin'					
Ortho 5-Ply	Orthophthalic	'Fine' 500	2500	3.18	0.07
Iso 5-Ply	Isophthalic	'Fine' 500	2500	3.16	0.06
Iso Coarse 5-Ply	Isophthalic	'Coarse' 500	2500	3.08	0.03
Ortho 3-Ply	Orthophthalic	800	2400	3.06	0.05
Iso 3-Ply	Isophthalic	800	2400	2.89	0.11
			Average:	3.07	
'Medium'					
Ortho 10-Ply	Orthophthalic	'Fine' 500	5000	6.15	0.05
Iso 10-Ply	Isophthalic	'Fine' 500	5000	6.54	0.10
Iso Coarse 10-Ply	Isophthalic	'Coarse' 500	5000	6.12	0.04
Ortho 6-Ply	Orthophthalic	800	4800	5.67	0.04
Iso 6-Ply	Isophthalic	800	4800	5.77	0.08
			Average:	6.05	
'Thick'					
Ortho 15-Ply	Orthophthalic	'Fine' 500	7500	9.43	0.03
Iso 15-Ply	Isophthalic	'Fine' 500	7500	9.96	0.07
Ortho 9-Ply	Orthophthalic	800	7200	7.40	0.05
Iso 9-Ply	Isophthalic	800	7200	8.35	0.07
			Average:	8.84	

Table 1. Panels laminated

A Rosand IFW5 instrumented falling weight impact test machine was used for the impact testing. The test specimens are clamped between two steel `picture frames' of internal dimensions 120 mm × 75 mm, with the flat moulded face of the specimen facing down. A pneumatic cylinder applies a high clamping force via a long lever arm to the top clamping plate, and the bottom plate is secured to a solid supporting anvil. A 20 mm diameter steel impactor cylinder with a hemispherical end is connected to the bottom of a weight via an accurately calibrated load cell. This assembly is hauled to a prescribed height (corresponding to a prescribed incident energy) and then dropped down guide rails onto the specimen. Removable weights allow limited variation of the mass and hence the incident energy for a given velocity (or vice versa). An optical gate measures the incident impact velocity and starts the data capture. Software then calculates velocity, displacement and energy absorbed through successive integrations of the load-cell force–time data. Force was sampled 1000 times over 10 and 20 ms for the thicker and thinner specimens respectively. A low-pass filter of 2 kHz was used.

Tests were performed for a series of increasing incident energies from 0.5 up to 85, 195 and 190 J for the 3- and 5-ply, 6- and 10-ply, and 9- and 15-ply specimens respectively. A mass of 10.853 kg was used for all tests, except for the lowest incident energy drop for each panel where a mass of 2.853 was used to give a feasible drop height.

3. Results

Although there were differences between the damage suffered by the specimens from each panel, the main features followed a common trend as the incident energy was increased:

(i) For the very lowest energies no damage was visible.

(ii) A central circular internal delamination occurred at a very low threshold value. This delamination expanded, and was then accompanied by surface micro-buckling of the top-ply rovings, permanent indentation under the impactor, and matrix cracking on the back face.

(iii) Fibre fracture and further matrix degradation occurred in the centre of the back face. For the thicker laminates the top face and internal delaminations became rectangular or diamond shaped and then irregular. Smaller areas of delamination were seen for the thinner specimens, even when the maximum incident energies achievable by the machine were sufficient to give perforation failure.

Hence, the damage may be classified into three distinct stages corresponding to low, medium and high incident energies, which have been defined here as `un-delaminated', `internal delamination' and `fibre damage' respectively. As examples of fairly well developed damage, impacted 5- and 10-ply `Iso Coarse' specimens are shown in Figs. 1 and 2 respectively. Since the impact response of the thin laminates differed significantly from that of the medium and thick laminates the two types of behaviour are described separately in the following sections.

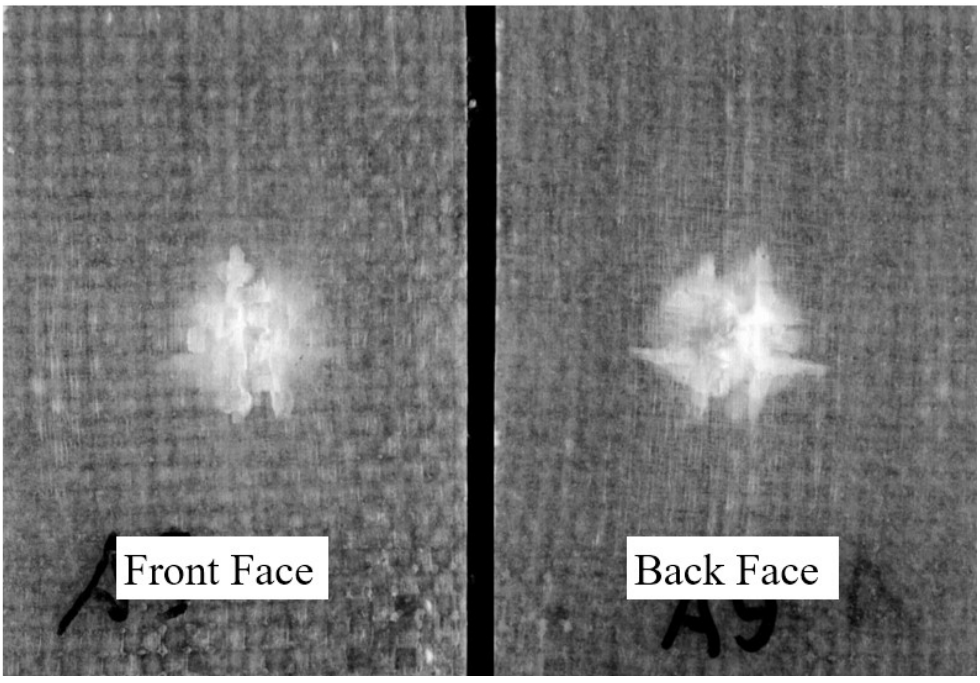

Fig. 1. Impact damaged 5-ply specimen.

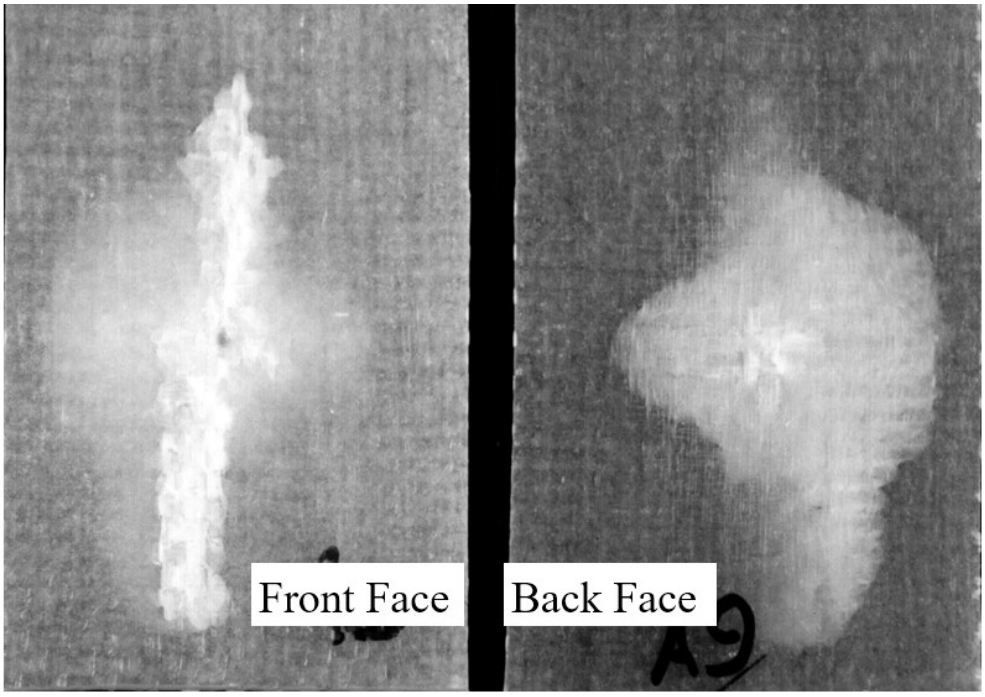

Fig. 2. Impact damaged 10-ply specimen.

3.1. Medium and thick laminates

Force–time and force–displacement plots summarise concisely the impact response. Fig. 3 is shown as an example of these responses for the medium and thick specimens for increasing incident energies. The force–deflection plots have a bi-linear form, the initial stiffer part corresponding to the response of the undelaminated specimen (c.f. (i) above). The force–time plots here are symmetrical and of identical duration, as would be expected for the undamaged case. As the incident energy is increased there is a sudden reduction in the stiffness of the specimen as an internal delamination occurs (c.f. (ii) above). A marked increase in impact duration accompanies the onset of this damage. However, considering that the slope of the force–deflection plots is more than halved after the onset of delamination, this increase in impact duration is not large. Despite the extension of the delamination with further increase in incident energy, the slope of the second part of the bi-linear force–deflection plot remains approximately constant, although the impact duration does increases slightly. The onset of fibre damage (c.f. (iii) above) is indicated by a saw-tooth pattern in the plots at higher incident energies.

Fig. 4 illustrates a significant variation on the response shown in Fig. 3. Although the overall behaviour is very similar, in Fig. 4 the onset of delamination is more prominent with an unstable increase in deflection at constant or even decreasing force, and a stronger associated step increase in the impact duration. All of the laminates reinforced with the higher-crimp 500 g m^{-2} woven roving (`Ortho 10-Ply', `Iso 10-Ply', `Ortho 15-Ply' and `Iso 15-Ply') show a response as in Fig. 3. Laminates of isophthalic resin reinforced with lower-crimp reinforcement (`Iso Coarse 10-Ply', `Iso 6-Ply' and `Iso 9-Ply') behave as shown in Fig. 4. The laminates of orthophthalic resin reinforced with lower-crimp reinforcement show a mixed response: `Ortho 6-Ply' as in Fig. 3 and `Ortho 9-Ply' as in Fig. 4.

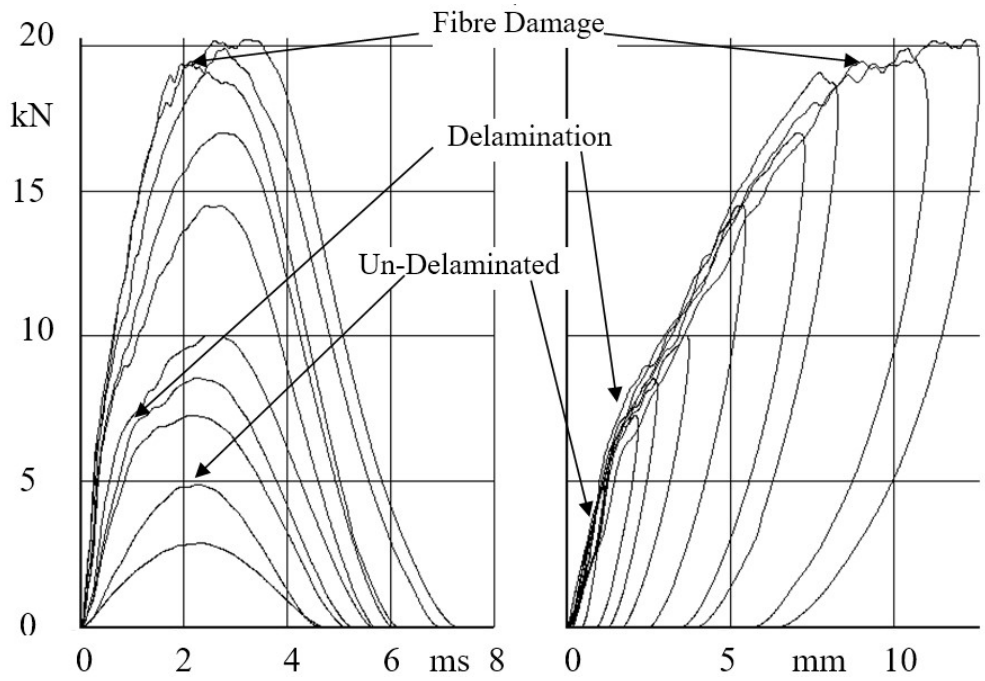

Fig. 3. `Ortho 15-ply' force–time and force–deflection plots.

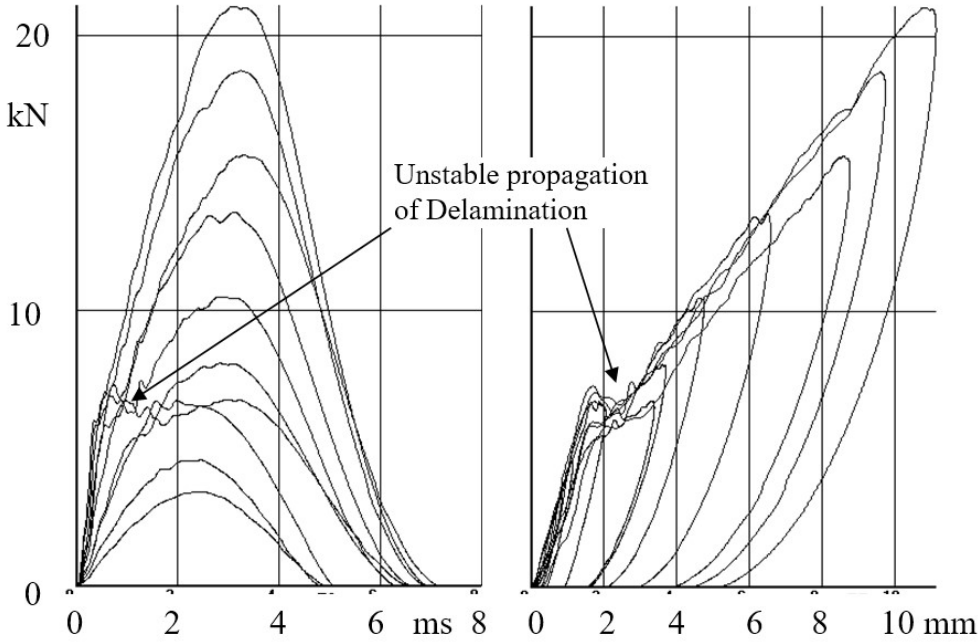

Fig. 4. `Iso 9-ply' force–time and force–deflection plots.

A trend in the variation of impact duration with incident energy is apparent in Figs. 5 and 6. Durations are lower at the lowest incident energies corresponding to the stiffer, undamaged specimens, and increase as delamination occurs. This is followed by a section of approximately constant or only slightly increasing duration corresponding to the internal delamination stage. It is also possible to see the effects of fibre damage at the highest incident energies where the impact duration rises as the laminates loose structural rigidity and penetration leads to perforation. This last point is more evident in Fig. 5 than in Fig. 6 since the maximum incident energy of the test machine was not always high enough to

give significant perforation of the thickest specimens. The incident energy at which fibre damage occurs varies from laminate to laminate, as discussed further below.

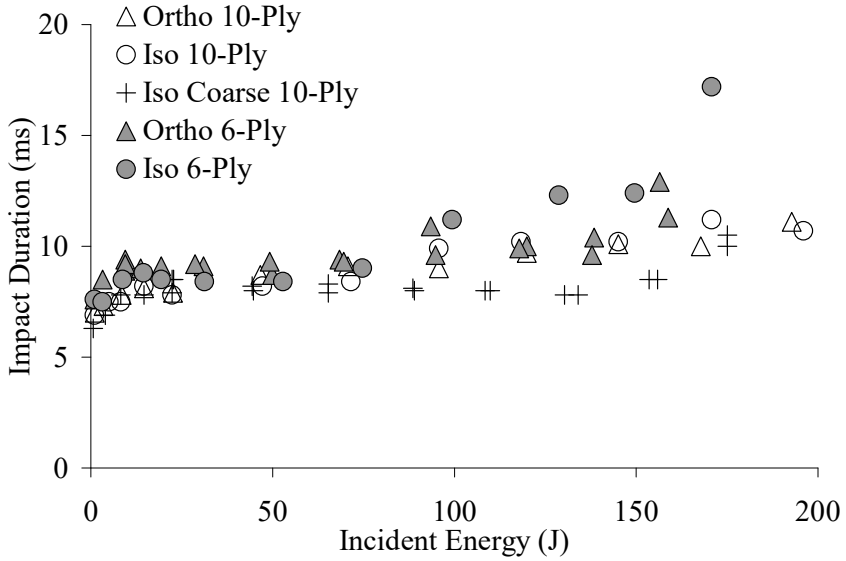

Fig. 5. Medium laminates impact durations.

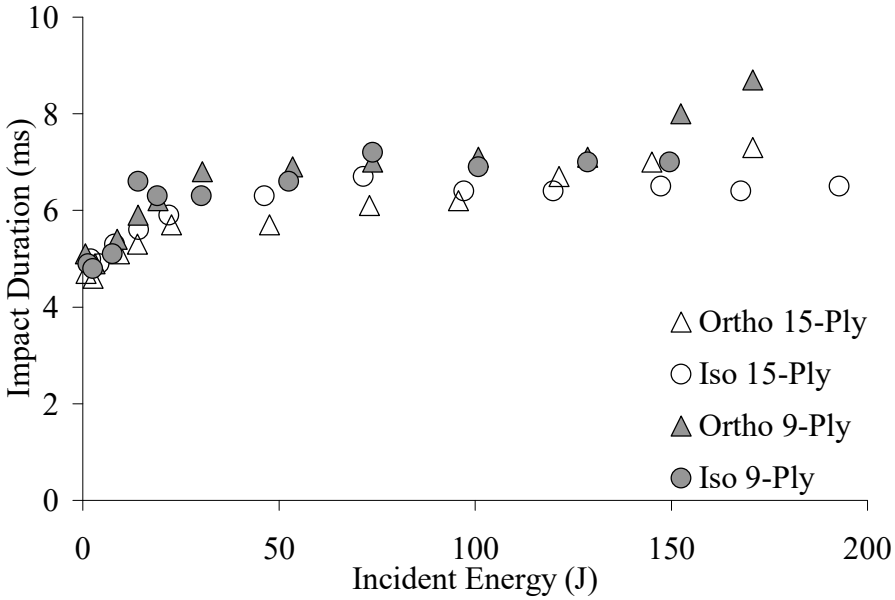

Fig. 6. Thick laminates impact durations.

Figs. 7 and 8 show how much incident energy has been irreversibly absorbed by the specimen at the end of the test for the medium and thick laminates respectively. Damage provides an important mechanism for this energy absorption. However, the work concerning circular plates [21] shows that even at incident energies too low to give significant damage a significant proportion of the incident energy is irreversibly absorbed by the laminate. The mechanisms responsible for this have not yet been confirmed, but probable explanations include hidden damage such as matrix micro-cracking, and/or visco-elastic and friction effects. The very low delamination initiation energies seen here mean

that little un-delaminated data is available in this study and further work is required to investigate this.

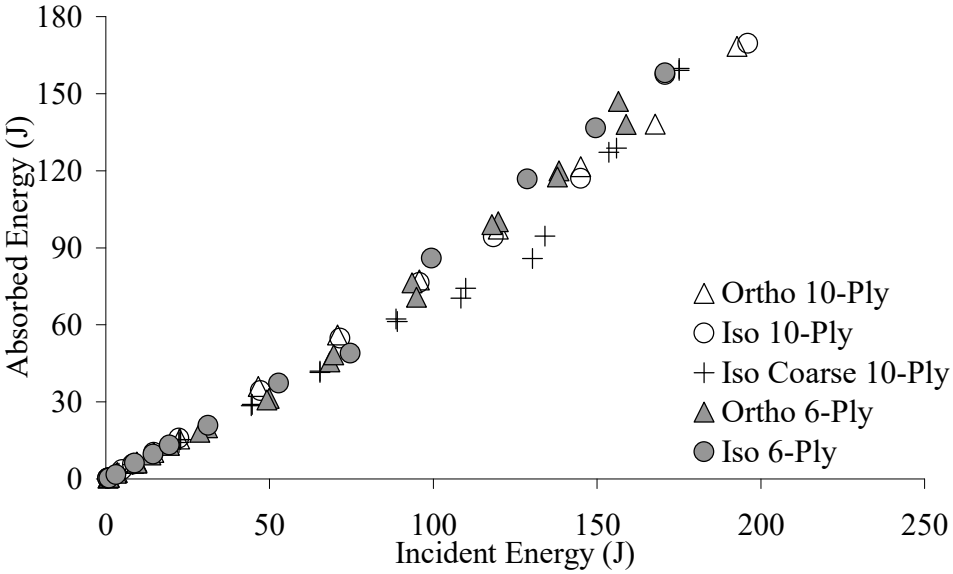

Fig. 7. Medium laminates absorbed energy.

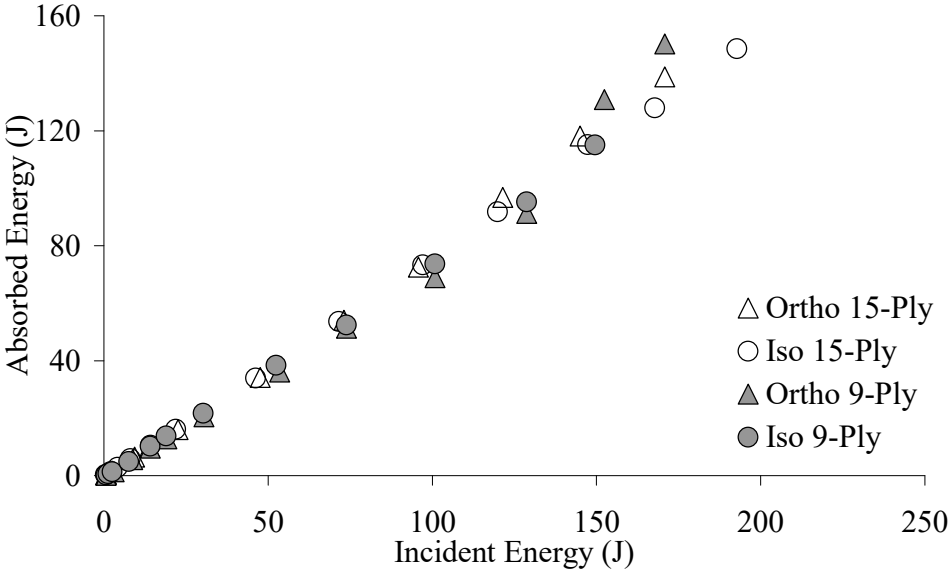

Fig. 8. Thick laminates absorbed energy.

The onset of fibre damage is evident in these plots, although the maximum incident energy of the test machine again limits the appearance of this in Fig. 8. Initially a linear relationship is seen where approximately two-thirds of the incident energy is absorbed. The point at which this slope increases further coincides with the onset of energy absorbing fibre damage as a precursor to perforation and/or shear failure. A coarser weave, lower-crimp reinforcement appears to delay the onset of fibre damage.

3.2. Thin laminates

Fig. 9 is given as an example of the impact response of the thin laminates. Although delamination also occurred at a low threshold value of incident energy for these specimens

there is no bi-linear response demarking the undamaged and internal delamination behaviours as for the medium and thick specimens. At higher incident energies, and hence higher deflections, fibre damage is again reflected in a `saw-tooth' pattern in the plots.

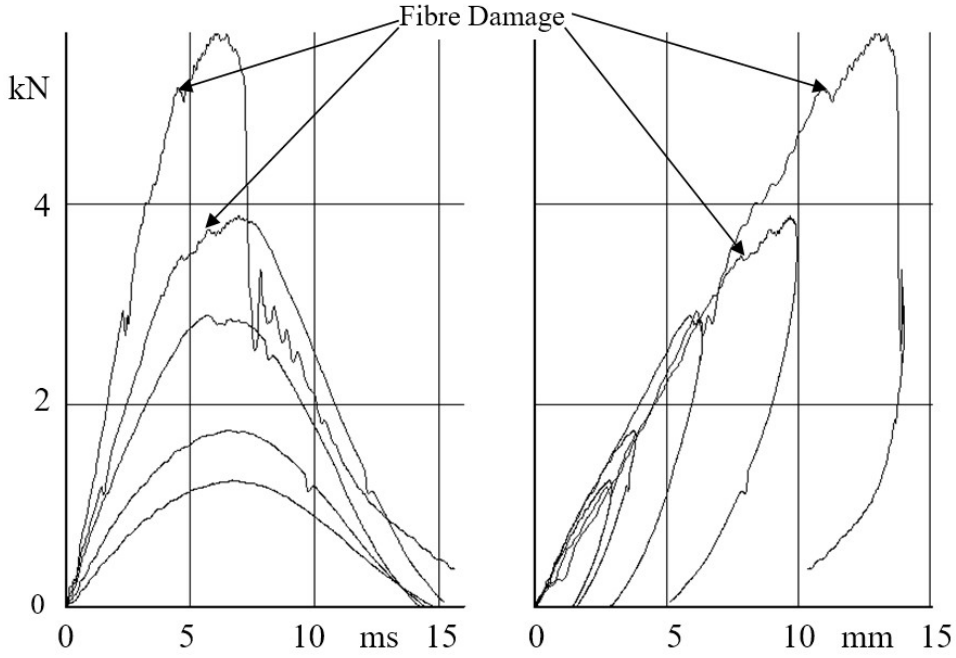

Fig. 9. `Ortho 5-ply' force–time and force–deflection plots.

Fig. 10 shows a significant variation on the thin laminate response shown in Fig. 9. As the incident energy and hence the deflections increase the plots for each test curve upwards. This is thought to be as membrane effects become important, before fibre damage becomes significant. In Fig. 9 fibre damage occurs before any membrane effects can become significant. These membrane effects are only seen for the lower-crimp woven roving reinforced laminates (`Iso 5-ply Coarse', Ortho 3-ply' and `Iso 3-ply').

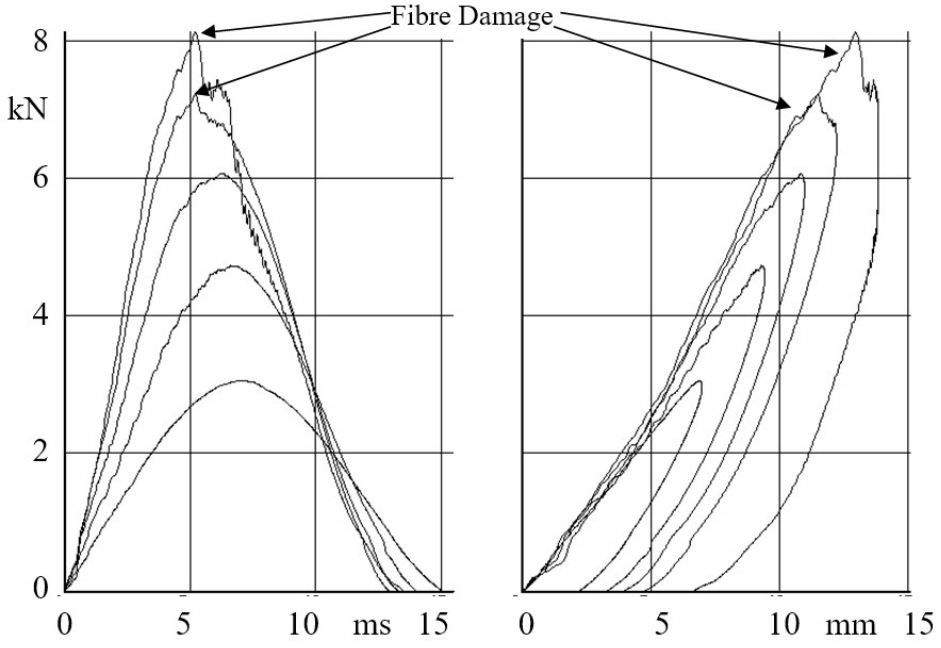

Fig. 10. `Iso 5-ply Coarse' force–time and force–deflection plots.

It is also thought that some form of effect of strain rate is also active. Membrane effects alone do not explain the fact that the increase of stiffness with deflection is greater for those tests at the higher incident energy. Since the durations of the high and low energy tests are very similar but the former tests reach higher deflections, higher strain rates are seen for the higher impact energies. This effect could be due to rate dependant material properties, but could also be due to delamination propagation rate effects.

Fig. 11 shows the impact duration of the thin laminates. Contrary to the data for the thicker laminates, an initial shortening of duration with increasing incident energy is seen here. This drop in duration is slight except for the `Iso 5-ply' and the `Ortho 3-ply' laminates where it is marked. Durations then remain approximately constant until rising as fibre damage starts. The effect of fibre damage may be seen in the absorbed energy plot in Fig. 12, and again the general trend is that the onset of fibre damage is delayed by the use of lower-crimp reinforcements. At lower incident energies, as for the medium and thick laminates, there is a linear relationship between absorbed and incident energy, again with a slope of approximately two thirds.

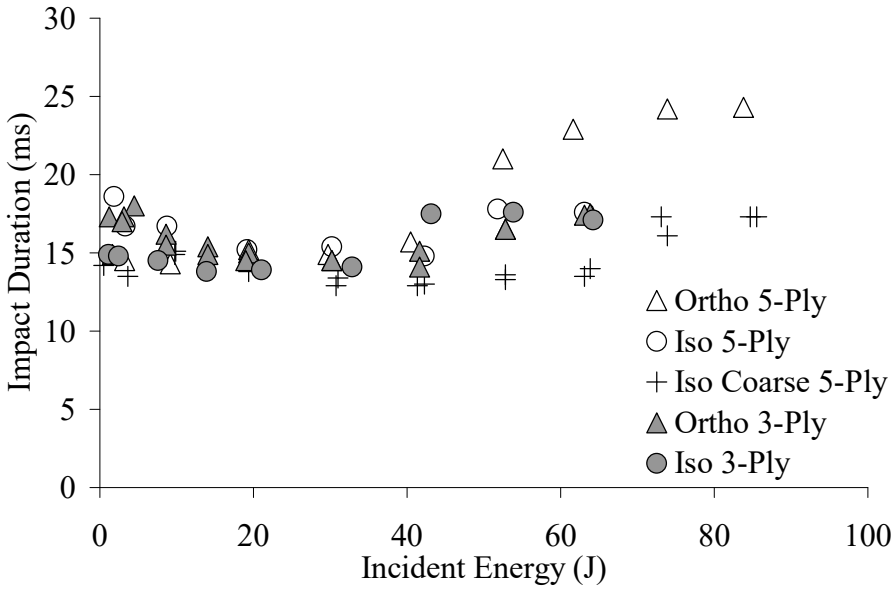

Fig. 11. Impact durations of thin laminates.

4. Analysis

The modelling of the case studied here presents a challenging analytical problem. The solutions to the static response of centrally loaded rectangular isotropic materials for small deflections are complex but well known [22,23]. However, the present case considers not only the dynamic contact response of an anisotropic material, but both large deflection and transverse shear effects are also significant, giving a highly complex non-linear problem. Most importantly, multiple, interacting and progressive damage modes are present even for the lowest incident energies and the damage path itself is sensitive to many factors including constituent materials used, their specific forms and surface treatments and the composite architecture. The laminate production method is also significant, and the inherently variable hand lay-up method considered here introduces a random element to

laminate properties, such as fibre and void content and reinforcement geometry, which vary both within and between panels.

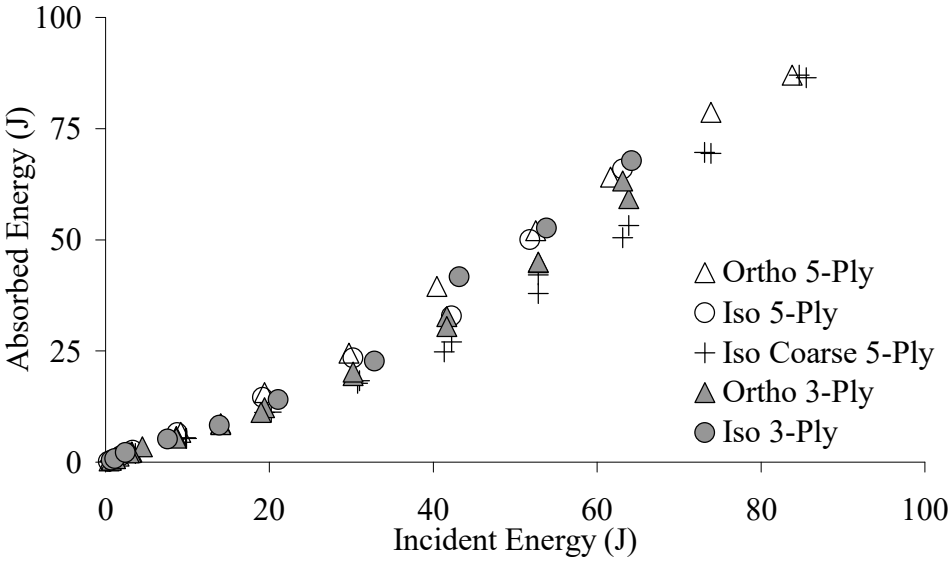

Fig. 12. Thin laminates absorbed energy.

It becomes clear that any attempt to model exactly the behaviour considering all of the above points quickly becomes extremely, if not intractably, complex. Also, many of the material property values essential as input into such detailed models are often either not available and/or extremely difficult to measure accurately. Further, any such model will be only applicable to the exact specific material system considered (even between nominally identical raw materials from different suppliers) and so the practical use of such an approach is at best questionable. Here the approach taken was to ask the question, `How can the large amount of data that accompanies impact testing be simply and concisely presented enabling us to identify the different processes occurring?' To achieve this a greatly simplified model has been applied to the data and deviations from the model used to identify significant features of the complex behaviour observed. This identification and separation of the various significant behaviours from the overall complex impact response is an essential first step in directing future work to further investigate the mechanisms thought to be responsible.

4.1. Force–deflection relationship

As shown in Section 3, force–time and force–displacement plots summarise concisely the impact response. The force–deflection relationship may be written as [24]:

$$P = K_{bs} w + K_m w^3 \qquad (1)$$

where the effective stiffness due to bending and shear k_{bs} is given by

$$K_{bs} = \frac{K_b K_s}{K_b + K_s} \qquad (2)$$

The subscripts b, s and m for the stiffness *K* refer to bending, shear and membrane respectively.

Shivakumar et al. [24] provide expressions for the stiffness' of a circular, centrally loaded composite plate of the forms:

$$K_m = A_o h; \quad K_b = B_o h^3; \quad K_s = C_o h \qquad (3)$$

where h is the plate thickness and A_0, B_0 and C_0 are terms involving only laminate material properties and plate radius.

For a given composite material and plate diameter, A_0 and B_0 may be considered as constants, as may C_0 assuming that the contact radius does not vary significantly. Here the assumption is made that stiffness equations of the same form as in Eq. (3) may be applied to the rectangular plate geometry considered here. It is also assumed that indentation for these relatively flexible specimens is not significant in comparison to deflections due to bending and shear.

Previous work on nominally identical materials [15,20] and that of Zhou and Davies [25] concerning similar laminates (but of a much higher fibre fraction) suggest that shear deflections dominate, especially when damage is present. Assuming the membrane term in Eq. (1) can be ignored, and combining Eqs. (1)–(3) gives:

$$\frac{P}{h} = C_o \left(\frac{h^2}{h^2 + C_o / B_o} \right) w \qquad (4)$$

For thick plates, or when the combination of material properties and plate diameter mean that $C_0 \ll B_0$, shear deflections will be much larger than those due to bending and hence Eq. (4) reduces to the simple equation:

$$\frac{P}{h} \approx C_o w \qquad (5)$$

Hence, Eq. (4) shows that if shear and bending deflections dominate then plots of force normalised by thickness against deflection should yield linear relationships whose slopes increase with laminate thickness. Further, Eq. (5) shows that if only shear deflections dominate a similar plot will also lead to linear relationships, but whose slopes are in this case independent of laminate thickness.

Maximum force normalised by thickness is plotted against deflection at maximum force for the thin, medium and thick specimens in Figs. 13–15 respectively. Since tests were carried out at a range of increasing incident energies the maximum values for each test may be plotted to give a clearly presentable summary of all data on the same plot. R^2 is the statistical `goodness of fit' parameter for the linear trends (0 corresponding to no linearity, 1 to a highly linear trend). To facilitate comparisons between each laminate thickness, broken lines indicating the other laminate thickness best-fit lines have been included on each plot.

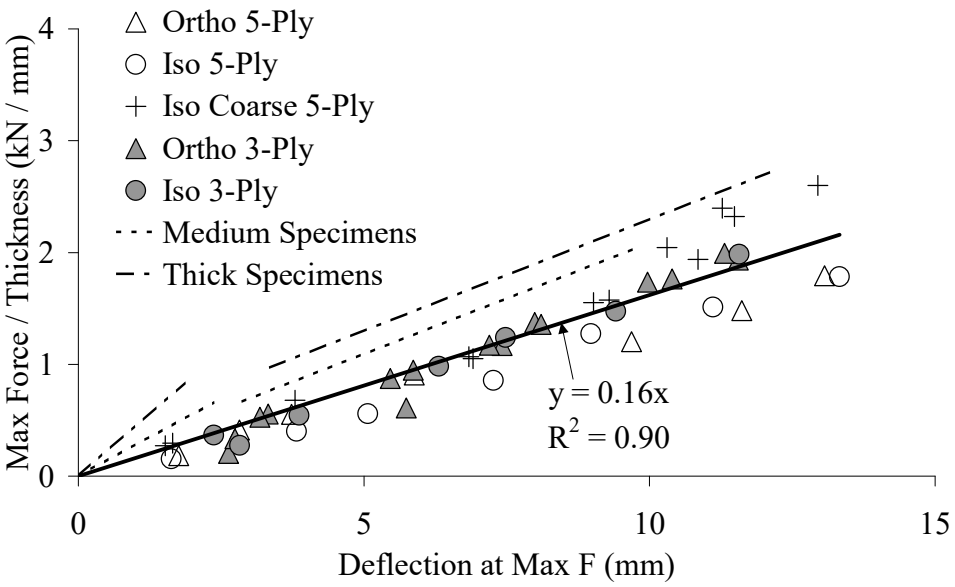

Fig. 13. Thin laminates maximum force/thickness vs. deflection.

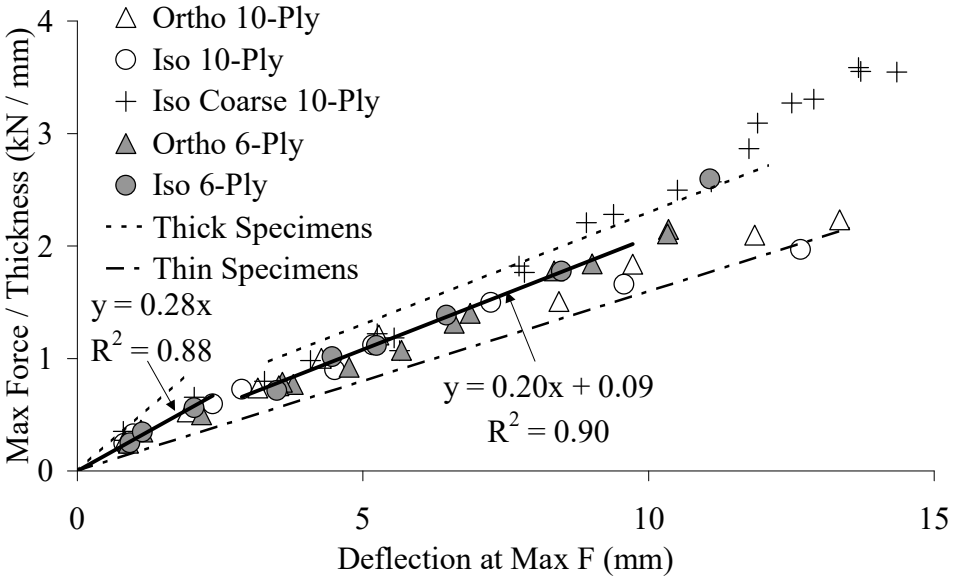

Fig. 14. Medium laminates maximum force/thickness vs. deflection.

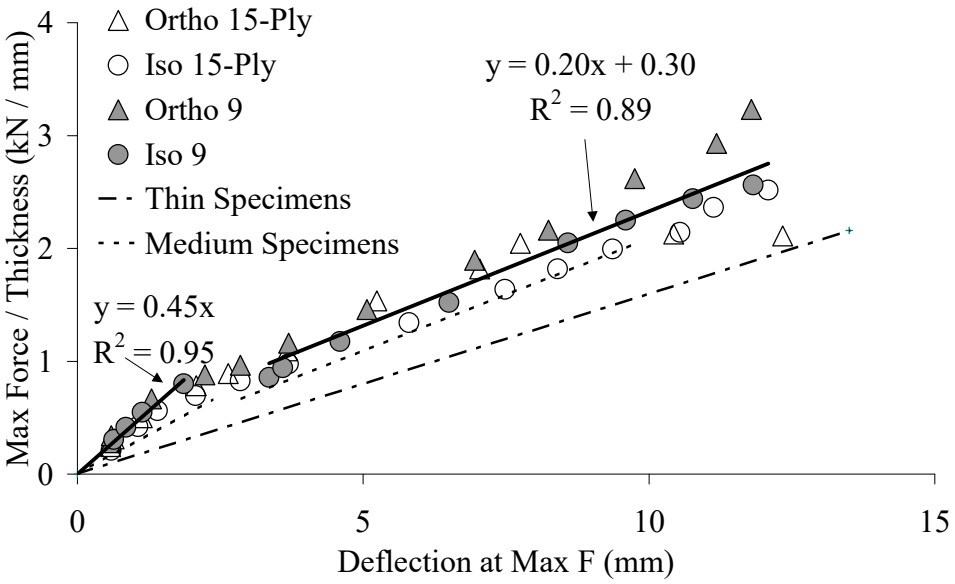

Fig. 15. Thick laminates maximum force/thickness vs. deflection.

Strong linear trends are seen in each plot. Reflecting the force–deflection behaviour discussed in Section 3, the medium and thick laminates show a bi-linear relationship due to the onset of delamination. However, a reduction in stiffness does not accompany the similar but less extensive delamination of the thin specimens in Fig. 13. The bi-linear relationships of Figs. 14 and 15 may be described by Eq. (6). The simple linear trend shown in Fig. 13 is described by Eq. (6a) for the whole range of displacements.

$$\frac{P}{h} = M_0 w \quad (a) \qquad \text{and} \qquad \frac{P}{h} = M_1 w + (M_0 - M_1) w_{crit} \quad (b) \qquad \textbf{(6)}$$
$$\text{for } w \le w_{crit} \qquad\qquad \text{for } w \ge w_{crit}$$

where M_0 and M_1 are the undamaged and delaminated gradients respectively, and w_{crit} is the deflection at the onset of delamination.

Comparing the undelaminated slopes, M_0 increases significantly with specimen thickness and this indicates that bending contributes significantly to the deflections (c.f. Eq. (4)). However, the delaminated slopes for the medium and thick laminates are equal implying that here shear deflections dominate (c.f. Eq. (5)). Hence, what may be regarded nominally as a simple bending controlled panel design problem will in fact lead to significant errors if shear effects are not considered in the calculations. The very early onset of delamination means that this shear-dominated behaviour affects the best part of the impact response. However, the lack of a reduction in stiffness with the onset of delamination for the thin specimens suggests that bending deflections dominate the response of the thinnest laminates even where delamination is present.

The increase in maximum force/thickness values at higher deflections for the coarse 500 g m^{-2} laminates and to a lesser extent by the 800 g m^{-2} laminates again indicate that these lower-crimp reinforcement give rise to membrane effects whereas these effects are not seen for the higher-crimp 500 g m^{-2} specimens. The absorbed energy and impact duration

plots of Section 3 show that the onset of fibre damage is earlier for the higher-crimp laminates suggesting that at higher deflections fibre damage occurs (with the associated energy absorption and reduction in impact force) before membrane effects become significant. The exact damage paths leading to fibre damage are multiple, complex, interacting and require further investigation, but matrix and fibre damage on the back-face would be expected to occur at lower deflections as higher-crimp weaves `straightened-out' under in-plane tensile stresses. Similarly, the increased buckling instability of higher-crimp front-face plies would lead to earlier compression failure of these laminates.

4.2. Force–incident energy relationship

It is desirable to predict the impact response for a given incident energy since the latter is often used as a measure of the severity of an impact event. Considering the complexity of the analytical problem (as described at the beginning of this section) an energy balance approach is taken here. It is assumed that all incident kinetic energy (IKE) has been absorbed by the specimen at the maximum force as damage and potential energy due to the specimen stiffness and deflection. Calculating the energy absorbed by integration of the force–deflection response, equating this to the IKE and normalising both sides by thickness gives:

$$\frac{IKE}{h} = \int_0^{w_{PMax}} \frac{P}{h} dw \qquad (7)$$

Substituting for P/h from Eq. (6) into Eq. (7) and integrating gives:

$$\frac{IKE}{h} = \frac{1}{2}\left(M_1 w_{PMax}^2 + 2(M_o - M_1) w_{crit} w_{PMax} + (M_1 - M_o) w_{crit}^2\right) \qquad (8)$$

Rearranging Eq. (6) to give deflections in terms of force normalised by thickness and substituting into Eq. (8) gives the desired relationship between maximum force and incident energy;

$$\left(\frac{P_{Max}}{h}\right)^2 = 2M_o\left(\frac{IKE}{h}\right) \qquad (a)\ for\ IKE \le IKE_{crit}$$

$$\left(\frac{P_{Max}}{h}\right)^2 = 2M_1\left(\frac{IKE}{h}\right) + \left(\frac{M_o - M_1}{M_o}\right)\left(\frac{P_{crit}}{h}\right)^2 \qquad (b)\ for\ IKE \ge IKE_{crit} \qquad (9)$$

where IKE_{crit} and P_{crit} are the incident energy and impact force at the onset of delamination.

Hence plots of $(P_{Max}/h)^2$ against (IKE/h) should give linear trends if bending and shear deflections are controlling. As in Section 4.1 significant bending will give an increase in slopes with thickness, but where shear deflections dominate slopes will be independent of thickness. The thin, medium and thick laminate data is presented accordingly in Figs. 16–18 respectively.

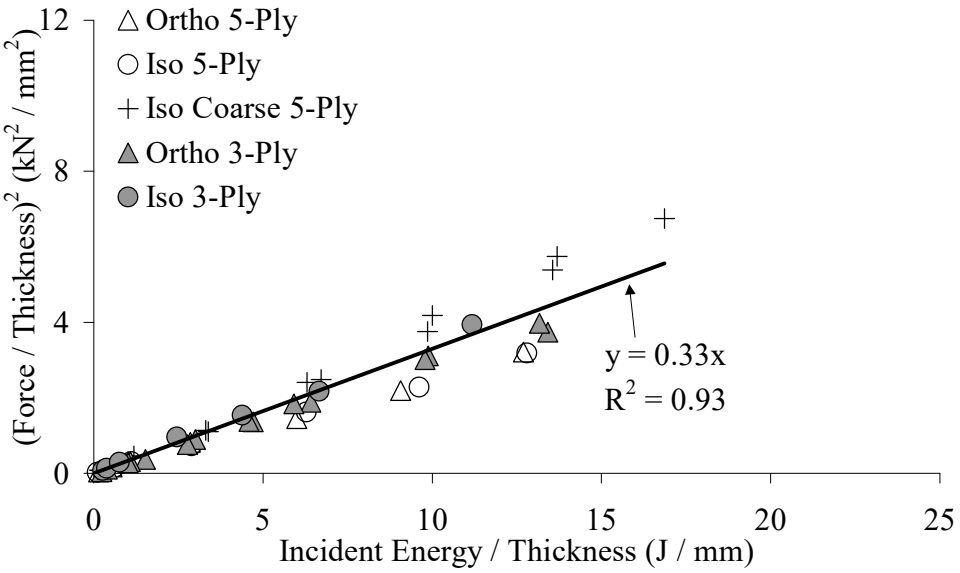

Fig. 16. Thin laminates force–IKE relationship.

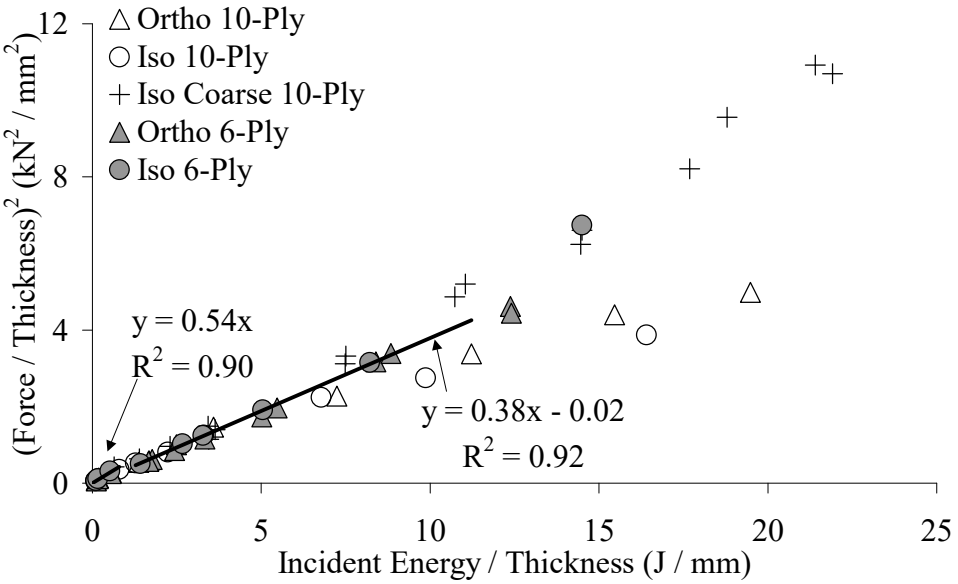

Fig. 17. Medium laminates force–IKE relationship.

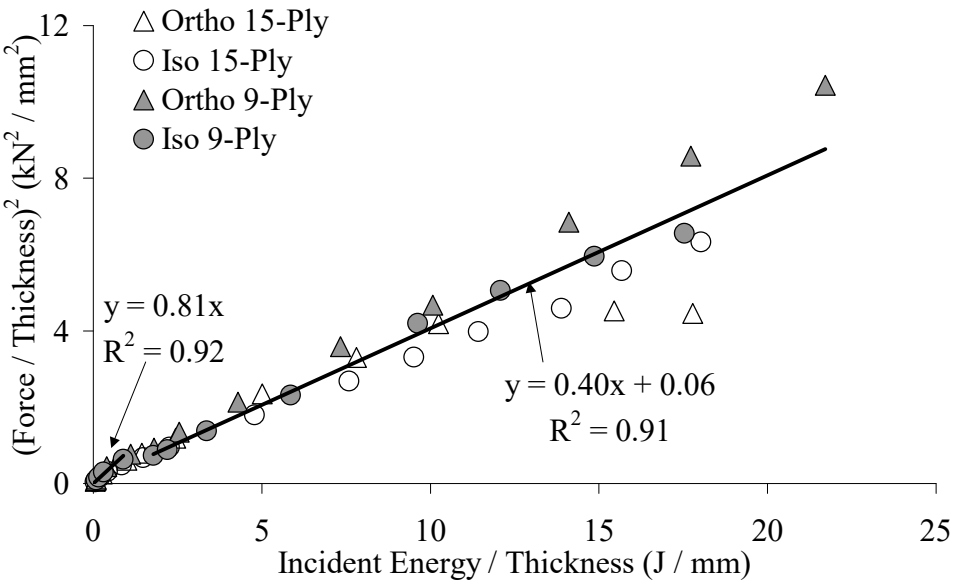

Fig. 18. Thick laminates force–IKE relationship.

Again, the high R^2 values show strong linear trends. The behaviour seen in Section 4.1 is reflected here with bi-linear behaviour for medium and thick laminates corresponding to undelaminated and delaminated behaviour. A simple linear relationship is again seen for the thin specimens although delamination did occur. Membrane effects are evident for the lower-crimp laminates at higher defections.

It is evident that in terms of incident energy the undelaminated behaviour of the medium and thick specimens is very short lived, and almost all of the impact response is delamination controlled. The increase in slope with specimen thickness for the thin laminates and the undelaminated medium and thick specimens again indicate that bending is significant. The very similar slopes of the delaminated medium and thick linear trends again indicate that shear deflections dominate here.

These plots show how a simple energy balance approach allows simple presentation of the impact response data in an easily interpreted form. Impact force as an intuitive measure of the impact response is given in terms of incident energy as a measure of the severity of the impact event. A simple theoretical approach leads to normalisation of the data by thickness, collapsing the data onto very similar linear trends, especially for thicker laminates.

5. Conclusions

The impact response of rectangular low fibre volume, hand laminated, woven-roving E-glass/polyester composite plates of differing thickness has been investigated using an instrumented drop-weight machine. Both orthophthalic and isophthalic resin, and different weights of woven roving with differing degrees of fibre crimp were considered.

The laminates exhibited damage even when subjected to impacts of very low incident energy. Multiple, complex and interacting damage mechanisms became more severe with increasing incident energy. Although there were differences between failure modes for different laminates and thickness, it was possible to characterise a common progression of three stages of damage with increasing incident energy; `undelaminated', `delaminated' and

`fibre damage'. The degree of fibre-crimp was thought to be more influential than the type of polyester resin used.

For the thicker specimens a higher stiffness at very low incident energies was suddenly reduced as delamination occurred giving a bi-linear force–deflection response. This was reflected in an increase in the duration of the impact event. For the thinnest laminates there was no equivalent change in stiffness, despite delamination at a low incident energy threshold. The onset of delamination was accompanied by sudden unstable delamination growth for specimens of isophthalic resin reinforced with lower fibre-crimp.

The onset of fibre damage was indicated by a jagged force–displacement response, an increase in the proportion of the incident energy irreversibly absorbed by the specimens and a corresponding increase in the impact duration. At higher deflections, lower fibre-crimp laminates showed a stiffening membrane effect, where some form of strain-rate dependant behaviour was also thought to be active. Fibre damage affected higher fibre-crimp laminates before such effects became apparent.

The assumption of a bending and shear deflection dominated model led to the concise presentation of the experimental data in the form of force normalised by thickness versus deflection plots. This graphical approach facilitated the identification and interpretation of the various types of impact behaviour. For thin and undelaminated thicker laminates bending was significant. However, for thicker delaminated laminates shear deflection dominated. Membrane effects were clearly identifiable as deviations from the linear theory.

An energy balance approach related the impact response to the severity of the impact event using plots of impact force squared against incident energy. Normalisation of the data by thickness collapses the data onto very similar linear trends, especially for thicker laminates. Delamination controls the impact response of thicker laminates for almost the whole range of incident energy until fibre damage occurs.

Acknowledgements

The first author has been financed by Fundação para a Ciência e a Tecnologia, Lisbon, Portugal, under contract number SFRH/BPD/1568/2000.

References

[1] Mouritz AP, Gellert E, Burchill P and Challis K. Review of advanced composite structures for naval ships and submarines. Composite Structures 2001;53:21-41.

[2] Richardson M.O.W. and Wisheart M.J. Review of low-velocity impact properties of composite materials. Composites Part A 1996; 27A: 1123-1131.

[3] Shyr T.W. and Pan Y.H. Impact resistance and damage characteristics of composite laminates. Composite Structures 2003;62:193-203.

[4] Cartié D.D.R. and Irving P.E. Effect of resin and fibre properties on impact and compression after impact performance of CFRP. Composites Part A 2002; 33: 483-493.

[5] Caprino G. and Lopresto V. On the penetration energy for fibre-reinforced plastics under low-velocity impact conditions. Composite Science and Technology 2001; 61: 65-73.

[6] Hirai Y., Hamada H. and Kim J.K. Impact response of woven glass-fabric composites – I. Effect of fibre surface treatment. Composite Science and Technology 1998; 58: 91-104.

[7] Christoforou A.P. Impact dynamics and damage in composite structures. Composite Structures 2001; 52: 181-188.

[8] Sutherland L.S. and Guedes Soares C. The effects of test parameters on the impact response of glass reinforced plastic using an experimental design approach. Accepted by Composites Science and Technology 2002.

[9] Abrate S. Impact on composite structures. Cambridge University Press, 1998.

[10] Sun C.T., Dicken A., Wu H.F. Characterization of impact damage in ARALL laminates. Composite Science and Technology 1993; 49: 139-144.

[11] Yang S.H., Sun C.T. Indentation law for composite laminates. ASTM STP 787 1982:425-449.

[12] Chen J.K., Sun C.T. Dynamic large deflection response of composite laminate subject to impact. Composite Structures 1985; 4(1): 59-73.

[13] Naik NK, Chandra Sekher Y and Sailendra Meduri. Damage in woven-fabric composites subjected to low-velocity impact. Composites Science and Technology 2000; 60:731-744.

[14] Abrate S. Modelling of impacts on composite structures. Composite Structures 2001; 51: 129-138.

[15] Sutherland L.S. and Guedes Soares C. Effects of laminate thickness and reinforcement type on the impact behaviour of e-glass/polyester laminates. Composites Science and Technology 1999;59:2243-2260.

[16] Caprino G., Langella A. and Lopresto V. Elastic behaviour of circular composite plates transversely loaded at the centre. Composites: Part A 2002;33:1191-1197.

[17] Caprino G., Langella A. and Lopresto V. Indentation and penetration of carbon fibre reinforced plastic laminates. Composites: Part B 2003;34:319-325.

[18] Berlingardi G. and Vadori R. Low velocity impact tests of laminate glass-fiber-epoxy matrix composite material plates. Int J Impact Eng 2002;27:213-229.

[19] Berlingardi G. and Vadori R. Influence of the laminate thickness in low velocity impact behavior of composite material plate. Composite Structures 2003;61:27-38

[20] Sutherland L.S. and Guedes Soares C. Impact tests on woven roving e-glass/polyester laminates. Composites Science and Technology 1999;59:1553-1567.

[21] Sutherland L.S. and Guedes Soares C. Impact characterisation of low fibre-volume glass reinforced polyester circular plates. Accepted by Int J Impact Eng 2003.

[22] Lukasiewicz S. Local loads in plates and shells. Sijthoff and Noordhoff, 1979.

[23] Timoshenko S.P. and Woinowsky-Krieger S. Theory of plates and shells. Mcgraw-Hill, 1959.

[24] Shivakumar K.N., Elber W. and Illg W. Prediction of impact force and duration due to low-velocity impact on circular composite laminates. J. Appl. Mech. 1985;52:674-680.

[25] Zhou G, Davies GAO. Impact response of thick glass fibre reinforced polyester laminates. Int J Impact Eng 1995;16(3):357-374.